

This is a provisional PDF only. Copyedited and fully formatted version will be made available soon.



ISSN: 0015-5659

e-ISSN: 1644-3284

Gallic acid treatment protects intestinal tissue against ischemia-reperfusion

Authors: Cemalettin Durgun, Engin Deveci

DOI: 10.5603/FM.a2023.0034

Article type: Original article

Submitted: 2023-01-03

Accepted: 2023-04-05

Published online: 2023-05-05

This article has been peer reviewed and published immediately upon acceptance. It is an open access article, which means that it can be downloaded, printed, and distributed freely, provided the work is properly cited.

Articles in "Folia Morphologica" are listed in PubMed.

Gallic acid treatment protects intestinal tissue against ischemia-reperfusion

Cemalettin Durgun, Engin Deveci, Gallic acid treatment protected intestine tissue

Cemalettin Durgun¹, Engin Deveci²

¹Division of General Surgery, Memorial Dicle Hospital, Diyarbakır, Turkey

²Department of Histology and Embryology, Faculty of Medicine, Dicle University, Diyarbakır, Turkey

Address for correspondence: Prof. PhD Engin Deveci, Department of Histology and Embryology, Faculty of Medicine, Dicle University, Diyarbakır, Turkey, e-mail: devecie32@hotmail.com

Abstract

Background: This study aimed to investigate the protective effects of gallic acid (GA) in the rat intestine against ischemia-reperfusion (IR) injury.

Materials and methods: Thirty male Wistar albino rats with a mean weight of 200–250 g were used. Animals were categorized into the sham, IR, and IR+GA groups. Ischemia of the intestine was induced for 3 h by occluding the superior mesenteric artery (SMA) and then left for 3 h of reperfusion. In the IR+GA group, after ischemia induction, 50 mg/kg GA was orally administered to the animals. Blood samples were collected for biochemical assays. Intestinal tissues were excised for histopathologic and immunohistochemical processing.

Results: Malondialdehyde (MDA) levels were increased, and catalase (CAT) and glutathione (GSH) levels were decreased in the IR group compared to the sham group. After GA treatment, MDA levels decreased and CAT and GSH levels increased in the GA-treated group compared to the IR group. In the sham group, normal intestinal histology was observed. In the IR group, the villi structures were completely degenerated. In the IR+GA group, histology was improved after GA treatment. In the sham group, the Caspase-3 reaction was generally negative in the epithelium and glands. In the IR group, the Caspase-3 reaction increased in apoptotic bodies and inflammatory cells. The Caspase-3 reaction was negative in goblet cells and the epithelium. A moderate Caspase-3 reaction was observed in the IR+GA group. The Beclin-1 reaction was negative in epithelial cells and goblet cells in villi in the sham group. In the IR group, the Beclin-1 reaction was positive in the degenerated villi. An intense Beclin-1 reaction was also observed in some inflammatory cells. After GA treatment, the Beclin-1 reaction was positive in a few cells. In general, moderate Beclin-1 positivity was observed.

Conclusions: GA, with its antioxidative effect, inhibited the apoptotic pathway (Caspase-3) through Beclin-1 regulation.

Key words: ischemia-reperfusion, gallic acid, Caspase-3, Beclin-1

INTRODUCTION

Intestinal ischemia-reperfusion injury is an event in which blood flow to the intestines is reduced and then restored to the ischemic tissue (1). Intestinal IR injury leads to severe local and systemic inflammation followed by damage to surrounding distant organs. Thus, the intestinal mucosal barrier is disrupted, and the organ is damaged. If this damage continues for a long time and is left untreated, the life of the animal may be endangered. Mortality rates vary between 60% and 80% in patients with acute intestinal IR; thus, new treatment strategies are needed for intestinal IR (2,3).

Gallic acid (GA; 3,4,5-trihydroxybenzoic acid) is a polyhydroxy phenolic compound, and structurally related compounds are widely found in fruits and plants. GA esters have diverse uses in industry, including as antioxidants in food, in cosmetics, and in the pharmaceutical industry. GA is a source material for inks, paints, and color developers. Studies have shown that these compounds are potential therapeutics, with anti-cancer and antimicrobial properties (4,5). GA was found to possess anti-inflammatory activity. Scavenging of superoxide anions, inhibition of myeloperoxidase release and activity, and interference with the assembly of active NADPH-oxidase may be the mechanisms underlying the inhibition of inflammatory process by GA (5).

Caspases are cysteine proteases that are involved in cell death. They play very important roles in embryonic development and cell homeostasis. Caspase-3, on the other hand, belongs to the effector caspase group and causes apoptotic cell morphology by degrading relevant proteins in the cell that will undergo apoptosis (6). Beclin-1 is a multidomain protein involved in autophagy mechanisms and membrane trafficking. It can also bind to B-cell lymphoma 2 to regulate apoptosis. Beclin-1 plays roles in tumorigenesis, neurodegeneration, and other diseases. The expression of Beclin-1 is affected by many other factors (7,8). Immunohistochemistry is a laboratory method used to detect the localization of specific antigens.

In this study, we aimed to investigate the effect of GA in rat intestinal tissue against ischemia and reperfusion with immunohistochemical and biochemical techniques.

MATERIALS AND METHODS

Animals

All experimental protocols were conducted according to the National Institutes of Health Guidelines for the Care and Use of Laboratory Animals. The study was approved by a local ethics committee. Thirty male Wistar albino rats with a mean weight of 200–250 g were used. They were housed in an air-conditioned room with a 12 h/12 h light/dark cycle and constant temperature (23 ± 2 °C) and relative humidity (65–70%).

Surgical procedure

All rats were fasted 12 h before the experiment. The rats were anesthetized with an intramuscular injection of ketamine (50 mg/kg; Ketalar, Parke Davis, Turkey) and xylazine (10 mg/kg; Rompun, Bayer AG, Germany) under aseptic conditions. The abdominal region was shaved, and a 2–3-cm abdominal midline incision was made. In the intestinal IR injury model, the superior mesenteric artery (SMA) was carefully blocked with a nontraumatic microvascular clamp. At the end of the ischemic period, the clamp was removed, and the mesenteric artery was released.

Sham group: animals were laparotomized without SMA occlusion.

IR group: 3-h ischemia was induced by SMA occlusion. The intestine was then reperfused for 3 h.

IR+GA group: After the IR procedure, 50 mg/kg GA was orally administered to the rats for 14 days.

At the end of the experiment, all animals were sacrificed. The jejunum tissues of all groups were removed, divided into two equal pieces, and stored under suitable conditions for biochemical and histopathological investigations.

Biochemical analyses

Blood samples were collected in tubes with a gel separator and centrifuged for 5 min at 1550 *g*. The supernatant plasma was removed and placed in polypropylene plastic tubes. The tubes were labeled with the appropriate sample name and type. Samples were stored at –80 °C for the determination of the malondialdehyde (MDA), glutathione (GSH), and catalase (CAT) levels. MDA levels were determined using the double heating method of Draper and Hadley (9). MDA values were expressed as nanomoles per gram (nmol/g) of wet tissue. The GSH activity was measured by the method of Paglia and Valentine (10). CAT values were measured by the method of Zhang et al. (11).

Histopathological analysis

Intestinal sections were obtained for histopathological analysis and fixed in 10% buffered formalin, dehydrated in ethanol (50% to 100%), purified in xylene, and embedded in paraffin. Sections (4–5 mm thickness) were cut and stained with Hematoxylin & Eosin. The sections were studied to assess the pathological changes in the gingiva tissue (12).

Immunohistochemical analysis

Formaldehyde-fixed tissue was embedded in paraffin wax for further immunohistochemical examination. Sections were deparaffinized in xylene and passed through a descending alcohol series. The antigen retrieval process was performed in citrate buffer solution (pH 6.0) for 15 min in a microwave oven at

700 W. Sections were allowed to cool at room temperature for 30 min and washed twice in phosphate buffered saline (PBS) for 5 min. Endogenous peroxidase blockage was performed in a 3% hydrogen peroxide solution for 7 min. The washed samples were incubated in Ultra V block (catalog no. TA-015UB, Thermo Fisher, USA) for 8 min. Blocking solution was removed from the sections, which were then incubated overnight at 4 °C with primary antibodies against Caspase-3, (catalog no. ab4051, Abcam, USA) and Beclin-1 (catalog no. 207612, Abcam, USA). After washing the sections in PBS, secondary antibody (TP-015-BN, Thermo Fischer, US) was applied for 20 min. The sections were washed in PBS for 2 × 5 min and then exposed to streptavidin-peroxidase (TS-015-HR, Thermo Fisher, USA) for 20 min. Sections washed with PBS were allowed to react with DAB (TA-001-HCX, Thermo Fischer, US) chromogen. Counterstaining with Hematoxylin & Eosin was performed, and after washing, the preparations were mounted. Sections were examined under a light microscope (Zeiss Imager A2, Germany) (13).

The quantification of histological and immunohistochemical parameters was performed blindly by two expert pathologists. The H-score (HS) was used to assess the outcomes of immunohistochemical staining. $HS = \sum(1 + i) \times \pi_i$, where “i” indicates the staining intensity (0 = no expression, 1 = light, 2 = medium, 3 = dense, and 4 = very dense) and “ π_i ” indicates the percentage of staining intensity (14). Results were presented as median (minimum-maximum) and statistical analysis was conducted.

Statistical analysis

Data were analyzed using IBM SPSS 25.0 software (IBM, Armonk, New York, USA). The Shapiro–Wilk test was used for data distribution analysis. The Kruskal–Wallis test was used for multiple comparisons, and the Mann–Whitney U test was used for within-group comparisons. $p < 0.05$ was considered statistically significant.

RESULTS

The statistical analysis of biochemical and histochemical parameters is shown in Table 1. MDA levels, histological scores of inflammation, dilatation, and Caspase-3 and Beclin-1 expression were higher in the IR group than the sham group. CAT and GSH levels and histological scores of epithelialization were significantly lower in the IR group than the sham group. After GA treatment, MDA levels, histological scores of inflammation, dilatation, and Caspase-3 and Beclin-1 expression decreased in the GA-treated group compared to the IR group, and this decrease was statistically significant. Similarly, CAT and GSH levels and histological scores of epithelialization statistically significantly increased in the IR+GA group compared to the IR group.

Table 1. Biochemical and histological parameters of the sham, IR, and IR+GA groups.

Parameters	Groups	n	Median (Min-Max)	Mean Rank	P-value
MDA	Sham	10	22.05 (14.98–46.28)	6.00	*p < 0.001
	IR	10	48.57 (24.68–64.51)	20.50	**p = 0.04
	IR+GA	10	36.58 (25.16–50.36)	15.75	
GSH	Sham	10	1.63 (1.42–1.76)	20.30	*p < 0.001
	IR	10	0.42 (0.13–1.18))	5.50	**p < 0.001
	IR+GA	10	1.38 (1.19–1.88)	20.50	
CAT	Sham	10	8.02 (5.47–8.63)	25.50	*p < 0.001
	IR	10	4.11 (2.08–4.98)	7.00	**p < 0.001
	IR+GA	10	6.48 (4.83–7.33)	15.50	
Epithelialization	Sham	10	2.00 (1.00–3.00)	29.75	*p < 0.001
	IR	10	0.50 (0.00–3.00)	8.00	**p < 0.001
	IR+GA	10	2.00 (1.00–3.00)	20.00	
Inflammation	Sham	10	0.00 (0.00–1.00)	6.50	*p < 0.001
	IR	10	2.50 (2.00–3.00)	23.50	**p < 0.001
	IR+GA	10	1.00 (1.00–3.00)	16.50	
Dilatation	Sham	10	0.00 (0.00–1.00)	6.50	*p < 0.001
	IR	10	2.00 (2.00–3.00)	22.50	**p < 0.001
	IR+GA	10	1.00 (1.00–3.00)	14.75	
Caspase-3 expression	Sham	10	0.00 (0.00–1.00)	6.50	*p < 0.001
	IR	10	2.00 (2.00–3.00)	24.00	**p < 0.001
	IR+GA	10	1.00 (1.00–3.00)	16.00	
Beclin-1 expression	Sham	10	0.00 (0.00–1.00)	6.50	*p < 0.001
	IR	10	2.00 (2.00–3.00)	24.00	**p < 0.001
	IR+GA	10	1.00 (1.00–3.00)	14.50	

* Sham vs IR; ** IR vs IR+GA; MDA: Malondialdehyde, GSH: Glutathione, CAT: Catalase, IR: ischemia-reperfusion, GA: Gallic acid, n: number of animals

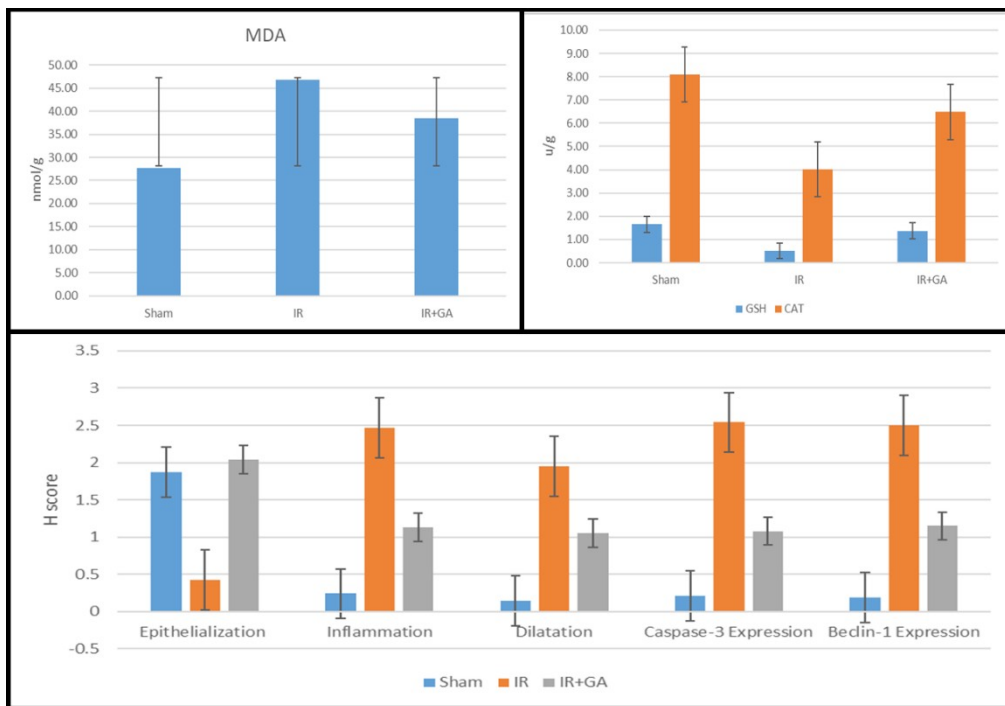


Figure 1. Graphical illustration of MDA, GSH, and CAT levels, epithelialization, inflammation, dilatation, and Caspase-3 and Beclin-1 expression.

Hematoxylin & Eosin findings

In the sham group, the transversal section showed that the villi structures of the intestine were regularly preserved, the goblet cells were regularly located in the epithelium, the prismatic appearance of the intestinal epithelial cells was smooth, and the connective tissue cells were freely distributed in the lamina propria in the lower parts. The muscle layer had a normal structure and the fibers extending from the lamina muscularis mucosal layer to the lamina propria were also in a smooth course. Vascular lumens were regular and endothelial cells were smooth (Figure 2a). In the IR group, the villi structures completely disappeared. Intense inflammation and cell infiltration was present between the muscle cells. Degeneration of goblet cells was found, and significant desquamation was observed in the intestinal epithelium. Degenerative and apoptotic changes were observed in the intestinal glands. Deterioration of the vascular structure and increased inflammation were observed. Mild hyperplasia was also observed in the muscles (Figure 2b). In the IR+GA group, the villi structures were found to be arranged in the form of leaves parallel to the lumen in the transversal section of the intestine, but desquamative cell debris was found at the ends. Cell degeneration was evident at the tip. Improvement was observed in goblet cells. Inflammatory cells in the lamina propria region showed a solitary distribution but did not increase much. The vascular structure was regular, and there were no degenerative changes in the endothelial cells. The muscle layer was smooth and circular (Figure 2c).

Caspase-3 immunostaining findings

In the sham group, although the villi structures were significantly preserved, the Caspase-3 reaction was generally negative in the epithelium and glands. The Caspase-3 reaction was found to be positive in some spilled parts but could be considered normal, and there was no apoptotic process. Additionally, towards the lamina propria and submucosa layer, some macrophage cells were concentrated, especially around the vessel, and showed positivity. A slight Caspase-3 reaction was also observed in the endothelial cells (Figure 2d). In the IR group, the integrity of the villi was completely lost. Breaks were also very evident in the underlying gland cells. In particular, the Caspase-3 reaction started to show significant positivity in the squamative cells in this direction. A significantly higher number of apoptotic areas were found, and intermediate inflammatory cells were also evaluated as positive for Caspase-3. Significant degenerative changes in the muscles were found with Caspase-3 positivity (Figure 2e). In the IR+GA group, the Caspase-3 reaction was clearly negative, especially in goblet cells and prismatic cells. Again, a moderate Caspase-3 reaction was observed in some of the gland cells, while the Caspase-3 reaction was widely evaluated as negative in the connective tissue cells in the lamina propria. The Caspase-3 reaction was positive in some cells in the submucosal region. In general, the apoptotic process was found to be weakened or decreased (Figure 2f).

Beclin-1 immunostaining findings

In the sham group, the Beclin-1 reaction was observed to be negative, especially in epithelial cells and goblet cells in the villi structures. Expression was also found to be negative in the underlying gland epithelium and goblet cells. Occasionally, the Beclin-1 reaction was found to be positive in some macrophages and inflammatory cells and in the lamina propria. The Beclin-1 reaction was negative in the muscle layer, but moderate Beclin-1 positivity was observed in some submucosal regions, especially around the vessel (Figure 2g). In the IR group, with the deterioration of the villi structures, the Beclin-1 reaction was positive, especially at the ends of the ruptured parts. An intense Beclin-1 reaction was also observed in some inflammatory cells in the lamina propria. The Beclin-1 reaction was found to be positive in degenerative gland cells close to the basement membrane and was also detected in inflammatory cells and vascular endothelium close to the muscle layer and submucosa region (Figure 2h). In the IR+GA group, the villi structure was preserved, and Beclin-1 expression was negative, especially in goblet cells. With the decrease in inflammatory structures, the Beclin-1 reaction was positive in a small number of cells. Particularly, moderate Beclin-1 positivity was observed in the vascular endothelium. Along with the represervation of the cell structure in some glands, the Beclin-1 reaction was observed to be positive in the cells that were degenerative from time to time. In general, moderate Beclin-1 positivity was noted (Figure 2i).

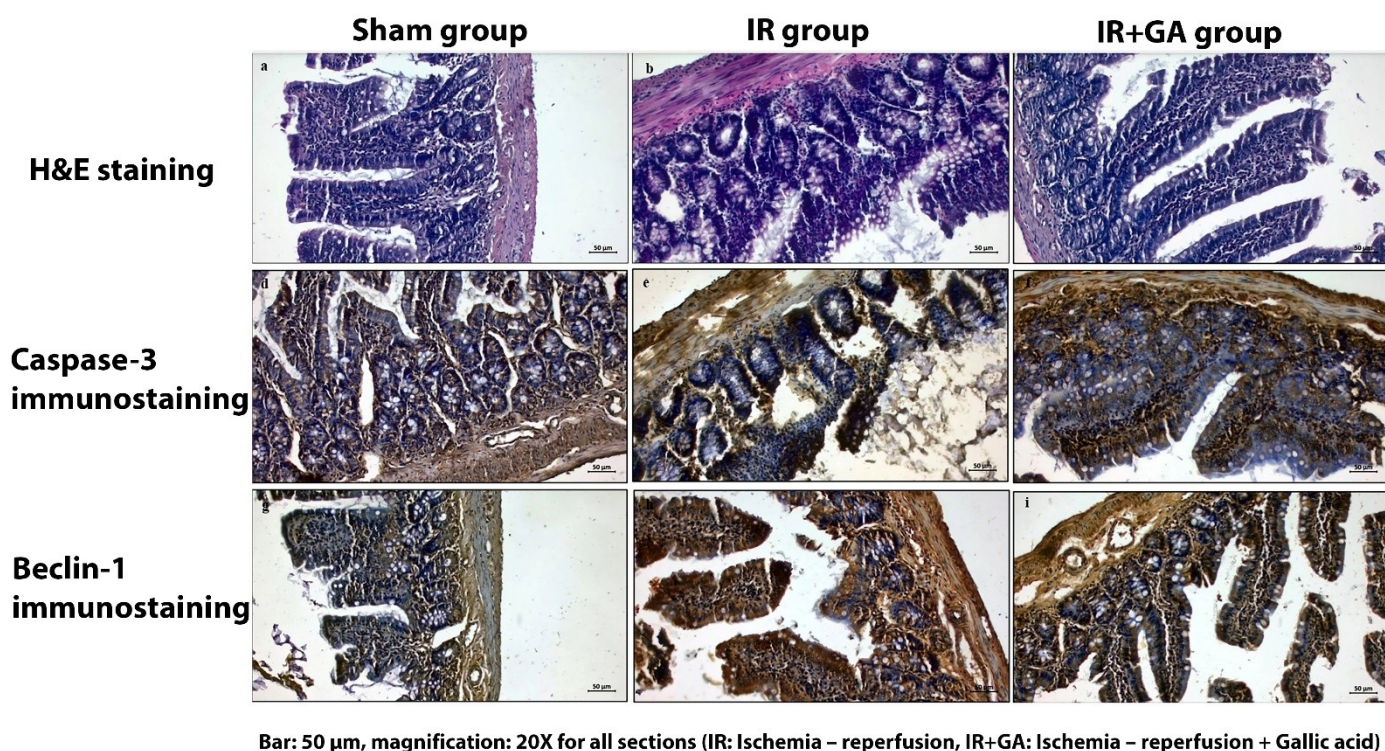


Figure 2. Hematoxylin & Eosin staining of intestinal tissue (**a**) sham group, **b**) IR group, **c**) IR+GA group). Bar: 50 μm, magnification: 20X. Caspase-3 immunostaining of intestinal tissue (**d**) sham group, **e**) IR group, **f**) IR+GA group). Bar: 50 μm, magnification: 20X. Beclin-1 immunostaining of intestinal tissue (**g**) sham group, **h**) IR group, **i**) IR+GA group. Bar: 50 μm, magnification: 20X.

DISCUSSION

Ischemia causes the insufficient delivery of oxygen and other metabolites by the circulation to the tissues, leading to cell death and organ failure. Reperfusion of the ischemic tissue may sometimes cause more harm than ischemia itself. During IR injury, the production of reactive oxygen species increases. MDA is an indicator of lipid peroxidation in tissues, and high levels of MDA are related to oxidative damage. The cell scavenges these harmful molecules using antioxidant enzymes such as superoxide dismutase, GSH, and CAT. During intestinal IR, the oxidant/antioxidant balance may change. Ji et al. studied the effects of intestinal IR on MDA and MPO levels and found that MDA and MPO levels increased in the IR group (15). Similarly, Chen et al. studied MDA, SOD, and GSH levels in intestinal IR injury and found that MDA levels increased in the IR group compared to the sham group, while SOD and GSH levels were lower in the IR group than in the sham group (16). The statistical analysis of biochemical and histochemical parameters in our study is shown in Table 1. MDA levels, histological scores of inflammation, dilatation, and Caspase-3 and Beclin-1 expression were higher in the IR group than the sham group. CAT and GSH levels and histological scores of

epithelialization were significantly lower in the IR group than the sham group. After GA treatment, MDA levels, histological scores of inflammation, dilatation, and Caspase-3 and Beclin-1 expression decreased in the GA-treated group compared to the IR group in a statistically significant manner. Similarly, CAT and GSH levels and histological scores of epithelialization statistically significantly increased in the IR+GA group compared to the IR group.

After rebleeding of the tissue, some cellular functions may be regained; however, rebleeding may cause more cellular damage. These changes affect the histology of intestinal tissue. Çimen et al. induced intestinal IR in rats and showed that IR injury caused polymorphonuclear leukocyte infiltration, edema, hemorrhage, vascular dilatation, and congestion in the IR group (17). Terzi et al. induced 60 min/60 min IR injury in the rat intestine and observed pathologies including desquamation in the epithelial layers, hemorrhage, and edema in the IR group (18). In our study, in the sham group, the villi structures of the intestine were regularly preserved, the goblet cells were regularly located in the epithelium, and the muscle layer had a normal structure (Figure 2a). In the IR group, the villi structures completely disappeared, and intense inflammation and cell infiltration was observed between the muscle cells. Goblet cells were degenerated, and significant desquamation was observed in the intestinal epithelium (Figure 2b). In the IR+GA group, the villi structures were arranged as normal, cell degeneration was decreased, goblet cells improved, inflammatory cells were decreased, and the vascular structure was regular (Figure 2c).

Caspases are cysteine proteases that are involved in cell death. They play very important roles in embryonic development and cell homeostasis. Caspase-3, on the other hand, belongs to the effector caspase group and causes apoptotic cell morphology by degrading relevant proteins in the cell that will undergo apoptosis. Li et al. (19) reported that Caspase-3 plays the most important role in the apoptotic process and that Caspase-9 has similar properties to Caspase-3. Kim et al. (20) studied cardiac IR and showed that oligonucleosomal deoxyribonucleic acid fragments were formed with the activation of Caspase-3, and the cell entered an irreversible pathway with the appearance of apoptotic bodies. Zhang et al. (21) showed that Caspase-3 messenger ribonucleic acid expression increased after IR injury in the rat lung. In our study, in the sham group, the Caspase-3 reaction was generally negative in the epithelium and glands and in other layers (Figure 2d). In the IR group, the Caspase-3 reaction increased in the apoptotic areas and intermediate inflammatory cells. Muscles showed Caspase-3 positivity (Figure 2e), while the Caspase-3 reaction was negative in goblet cells and the epithelium. A moderate Caspase-3 reaction was observed in some of the gland cells, while the Caspase-3 reaction was largely negative in connective tissue cells in the lamina propria (Figure 2f).

Autophagy is the lysosomal degradation of cell substances, which is key for maintaining cell homeostasis. Beclin-1 is a protein that regulates both apoptosis and autophagy. During IR, Beclin-1

expression is affected by many factors. Shi et al. (22) showed that Beclin-1 expression was especially upregulated during the reperfusion stage in myocardial IR injury. Luo et al. (23) found that Beclin-1 was overexpressed during cerebral IR injury and thus protected against neuronal death. Beclin-1 was also shown to protect against myocardial IR by regulating Caspase-4 expression (24). In our study, the Beclin-1 reaction was negative in epithelial cells and goblet cells in the villi structures. The Beclin-1 reaction was also negative in the muscle layer (Figure 2g). The Beclin-1 reaction was positive mainly in the ruptured villi. An intense Beclin-1 reaction was also observed in some inflammatory cells and degenerative gland cells (Figure 2h). The Beclin-1 reaction was positive in a small number of cells. In general, moderate Beclin-1 positivity was noted (Figure 2i).

There are limited clinical studies on the relationship between GA and Beclin-1 regulation at the apoptotic level. Huang et al. suggested that exposure to the GA-derived compound methyl gallate inhibits hepatocellular carcinoma proliferation both in vitro and in vivo. They also reported increased methyl gallate-induced cytotoxicity in hepatocellular carcinoma cells to block autophagy. Based on their findings, it has been suggested that methyl gallate may act as a powerful therapeutic for human hepatocellular carcinoma patients (25). Similarly, cells treated with propyl gallate, a derivative of GA, induced cell apoptosis, suggesting that it may be a new candidate for hepatocellular carcinoma therapy. The authors showed that propyl gallate inhibits hepatocellular carcinoma cell proliferation through enhanced reactive oxygen species production and autophagy activation (26).

CONCLUSIONS

IR caused cell degeneration, which activated a signal in the basal membrane accelerating the apoptotic process. Regulation of Beclin-1 was disrupted, and Caspase-3 was activated. GA reduced oxidative stress with its antioxidative effect and slowed down the apoptotic process mediated through the cell basal membrane with impaired Beclin-1 regulation. In addition, GA, which has an antioxidative effect in the IR model induced by SMA, has been experimentally shown to inhibit the apoptotic pathway (Caspase-3) through Beclin-1 regulation for the first time. In this respect, more experimental studies are needed.

REFERENCES

1. Klempnauer J, Grothues F, Bektas H, et al. Long-term results after surgery for acute mesenteric ischemia. *Surgery*. 1997; 121(3): 239-43, doi: 10.1016/s0039-6060(97)90351-2.
2. Wilcox MG, Howard TJ, Plaskon LA, et al. Current theories of pathogenesis and treatment of nonocclusive mesenteric ischemia. *Dig Dis Sci*. 1995; 40(4): 709-16, doi: 10.1007/BF02064966.

3. Kassahun WT, Schulz T, Richter O, et al. Unchanged high mortality rates from acute occlusive intestinal ischemia: six year review. *Langenbecks Arch Surg.* 2008; 393(2):163-71, doi: 10.1007/s00423-007-0263-5.
4. Ow YY, Stupans I. Gallic acid and gallic acid derivatives: effects on drug metabolizing enzymes. *Curr Drug Metab.* 2003; 4(3): 241-8 doi: 10.2174/1389200033489479.
5. Kroes BH, van den Berg AJ, Quarles van Ufford HC, et al. Anti-inflammatory activity of gallic acid. *Planta Med.* 1992; 58(6): 499-504, doi: 10.1055/s-2006-961535.
6. Porter AG, Jänicke RU. Emerging roles of caspase-3 in apoptosis. *Cell Death Differ.* 1999; 6(2): 99-104, doi: 10.1038/sj.cdd.4400476.
7. Tran S, Fairlie WD, Lee EF. BECLIN1: Protein Structure, Function and Regulation. *Cells.* 2021; 10(6): 1522, doi: 10.3390/cells10061522.
8. Menon MB, Dhamija S. Beclin 1 Phosphorylation - at the Center of Autophagy Regulation. *Front Cell Dev Biol.* 2018; 6: 137, doi: 10.3389/fcell.2018.00137.
9. Draper HH, Hadley M. Malondialdehyde determination as index of lipid peroxidation. *Methods Enzymol.* 1990; 186: 421-31, doi: 10.1016/0076-6879(90)86135-i.
10. Paglia DE, Valentine WN. Studies on the quantitative and qualitative characterization of erythrocyte glutathione peroxidase. *J Lab Clin Med.* 1967; 70(1): 158-69, PMID: 6066618.
11. Zhang C, Chen K, Wang J, Zheng Z, Luo Y, Zhou W, Zhuo Z, Liang J, Sha W, Chen H. Protective Effects of Crocetin against Radiation-Induced Injury in Intestinal Epithelial Cells. *Biomed Res Int.* 2020; 2020: 2906053, doi: 10.1155/2020/2906053.
12. Durgun C, Aşır F. Effect of ellagic acid on damage caused by hepatic ischemia reperfusion in rats. *Eur Rev Med Pharmacol Sci.* 2022; 26(22): 8209-8215, doi: 10.26355/eurrev_202211_30352.
13. Yaris M, Deveci E. Prophylactic Effect of *Potentilla fulgens* on Renal Ischemia-Reperfusion Injury in Rats. *Int J Morphol.* 2021; 39(1): 116-122, http://www.intjmorphol.com/wp-content/uploads/2020/12/art_18_391.pdf.
14. Taş F, Erdemci F, Aşır F, et al. Histopathological examination of the placenta after delivery in pregnant women with COVID-19 . *J Health Sci Med.* 2022; 5(3): 868-874, doi: 10.32322/jhsm.1100731
15. Ji YY, Wang ZD, Wang SF, et al. Ischemic preconditioning ameliorates intestinal injury induced by ischemia-reperfusion in rats. *World J Gastroenterol.* 2015; 21(26): 8081-8, doi: 10.3748/wjg.v21.i26.8081.
16. Chen R, Zhang YY, Lan JN, et al. Ischemic Postconditioning Alleviates Intestinal Ischemia-Reperfusion Injury by Enhancing Autophagy and Suppressing Oxidative Stress through the Akt/GSK-3 β /Nrf2 Pathway in Mice. *Oxid Med Cell Longev.* 2020; 2020: 6954764, doi: 10.1155/2020/6954764.
17. Çimen FK, Çimen O, Altuner D, et al. Effect of rutin on experimentally induced small intestinal ischemia reperfusion injury in rats: A biochemical and histopathological evaluation. *J Surg Med.* 2021; 5(1): 26-30, <https://dergipark.org.tr/tr/download/article-file/1501664>

18. Terzi A, Coban S, Yildiz F, et al. Protective effects of *Nigella sativa* on intestinal ischemia-reperfusion injury in rats. *J Invest Surg*. 2010; 23(1): 21-7, doi: 10.3109/08941930903469375.
19. Li M, Ona VO, Chen M, et al. Functional role and therapeutic implications of neuronal caspase-1 and -3 in a mouse model of traumatic spinal cord injury. *Neuroscience*. 2000; 99(2): 333-42, doi: 10.1016/s0306-4522(00)00173-1.
20. Kim GT, Chun YS, Park JW, et al. Role of apoptosis-inducing factor in myocardial cell death by ischemia-reperfusion. *Biochem Biophys Res Commun*. 2003; 309(3): 619-24, doi: 10.1016/j.bbrc.2003.08.045.
21. Zhang Z, Shen H, Qin HD, et al. Protective effect of N-acetylcysteine against pneumocyte apoptosis during ischemia/reperfusion injury of lung in rats. *Zhongguo Wei Zhong Bing Ji Jiu Yi Xue*. 2012; 24(2): 111-5, PMID: 22316545.
22. Shi B, Ma M, Zheng Y, et al. mTOR and Beclin1: Two key autophagy-related molecules and their roles in myocardial ischemia/reperfusion injury. *J Cell Physiol*. 2019; 234(8): 12562-12568, doi: 10.1002/jcp.28125.
23. Luo H, Huang D, Tang X, et al. Beclin-1 exerts protective effects against cerebral ischemia-reperfusion injury by promoting DNA damage repair through a non-autophagy-dependent regulatory mechanism. *Int J Mol Med*. 2022; 49(5): 61, doi: 10.3892/ijmm.2022.5117.
24. Sun W, Lu H, Dong S, et al. Beclin1 controls caspase-4 inflammsome activation and pyroptosis in mouse myocardial reperfusion-induced microvascular injury. *Cell Commun Signal*. 2021; 19(1): 107, doi: 10.1186/s12964-021-00786-z.
25. Huang CY, Chang YJ, Wei PL, et al. Methyl gallate, gallic acid-derived compound, inhibit cell proliferation through increasing ROS production and apoptosis in hepatocellular carcinoma cells. *PLoS One*. 2021; 16(3): e0248521, doi: 10.1371/journal.pone.0248521.
26. Wei PL, Huang CY, Chang YJ. Propyl gallate inhibits hepatocellular carcinoma cell growth through the induction of ROS and the activation of autophagy. *PLoS One*. 2019; 14(1): e0210513, doi: 10.1371/journal.pone.0210513.